Centrifugo-pneumatic valve for metering of highly wetting liquids on centrifugal microfluidic platforms†

Daniel Mark,*[a] Tobias Metz,[b] Stefan Haeberle,[a] Sascha Lutz,[a] Jens Ducrée,‡[a] Roland Zengerle[ab] and Felix von Stetten[ab]

Received 17th July 2009, Accepted 10th September 2009
First published as an Advance Article on the web 12th October 2009
DOI: 10.1039/b914415c

We designed and experimentally validated a new type of passive valve for centrifugal microfluidic platforms. A liquid column entering an unvented receiving chamber is stopped by the counter-pressure of compressed air. This valve opens under defined conditions at high centrifugal frequencies at which the interface between liquid and air becomes unstable and enables a phase exchange, forwarding the liquid. Burst frequencies of the valve were determined for liquids typically used in biochemical assays: pure water, water with detergent concentrations between 0.01 and 10%, and pure ethanol. Burst frequencies between 8.5 ± 0.6 and 27.9 ± 2.0 Hz were measured for different surface tensions. The burst frequencies can be tuned by simple geometrical changes in the valving structure. The valve does not require ultra-precise structures or local surface modifications and is therefore ideal for low-cost microfluidic polymer disks. Potential applications are in the field of multiparameter and panel analysis, such as PCR-genotyping.

Introduction

Microfluidic applications based on centrifugal actuation have the charm of relying only on one rotor as the sole actively actuated component.[1–7] They do not need any tubings to the macro-world and therefore promise to be very robust. A number of principles for passive valving structures which allow to steer the fluid flow by a centrifugation protocol have been introduced. Principles include hydrophobic patches,[7–9] geometrically defined capillary stops,[10,11] siphons,[12] wax valves[13,14] or fluidic capacitance switches,[15] each with its own area of applications and limitations. Hydrophobic patches are difficult to mass-produce since they require local surface modifications with high spatial resolution. Capillary stops are produced rather easily but provide very limited stopping power for liquids with low surface tension. Siphons stop liquids at high frequencies but can only be used with liquids in a certain contact angle range and require a lot of space which is often limited in centrifugal systems. Wax valves are quite universal but rather complex to produce and require an external energy source (*e.g.* laser). Fluidic capacitance switches are limited to certain protocols, since they require two separated liquid volumes. Overall, switching and stopping of highly wetting liquids with passive structures is an unsolved problem in centrifugal microfluidic systems. However, many analytical protocols, such as DNA extraction, require buffers containing high concentrations of detergents or ethanol.

In this study, we present a novel approach for a robust valve based on the compression of air by a liquid column, which also enables switching of liquids with low surface tension. Valves based on such a principle can have a very simple geometry and do not require local surface modifications or actuators on- or off-disk except for the disk drive. They are robust and very easy to produce and therefore decrease the overall complexity of the microfluidic system, thus adding a tool to the centrifugal microfluidic tool-box which is also suitable for inexpensive mass-production.

Working principle

The stopping effect of the presented centrifugal-microfluidic valve is based partly on surface tension (varies with liquid properties) but also air compression (independent of liquid properties). A suggested name for the structure is therefore "centrifugo-pneumatic valve".

The valving structure comprises a wide upstream channel, a narrow connecting channel and an unvented downstream receiving chamber (Fig. 1). Under centrifugation, the wide upstream channel fills with liquid, and air in this channel is displaced towards the center of rotation. Reaching the narrow connection channel, the liquid forms a meniscus that spans the entire narrow channel, preventing air from escaping the unvented receiving chamber. The advancing meniscus compresses the air in the chamber, until the generated air counter-pressure reaches an equilibrium with the centrifugally generated pressure in the liquid, effectively stopping the flow.

The liquid can be released into the receiving chamber by increasing the rotational frequency until liquid starts to "drip" into the receiving chamber (burst frequency). The entire liquid

[a]*HSG-IMIT – Institut für Mikro- und Informationstechnik, Wilhelm-Schickard-Straße 10, D-78052 Villingen-Schwenningen, Germany. E-mail: daniel.mark@hsg-imit.de*
[b]*Laboratory for MEMS Applications, Department of Microsystems Engineering - IMTEK, University of Freiburg, Georges-Koehler-Allee 106, D-79110 Freiburg, Germany*

† Electronic supplementary information (ESI) available: Details of measurement of surface tension and contact angles. Videos of filling of metering structure and of burst of valve. See DOI: 10.1039/b914415c

‡ This author is now employed at: Biomedical Diagnostics Institute, Dublin City University, Glasnevin, Dublin 9, Ireland.

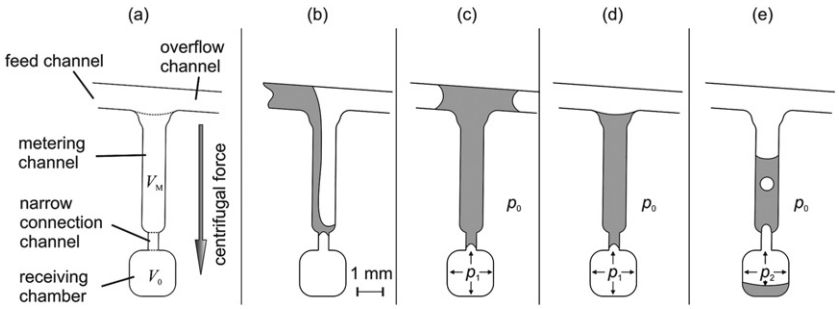

Fig. 1 A metering structure based on the centrifugo-pneumatic valve. (a) Nomenclature and volumes: Liquid can fill the metering channel through the feed channel. The metered volume is defined by the metering channel V_M, the volume of the receiving chamber is V_0. (b)–(e): Functional principle: (b–d) While liquid is filling the metering channel at a first centrifugal metering frequency, the increased air pressure p_1 stops the liquid from entering the receiving chamber. (e) At a higher centrifugal frequency, the liquid is transported to the receiving chamber while leaving air bubbles decrease the air pressure.

can be released despite the decreasing liquid plug length and increasing air pressure since the liquid/air interface becomes unstable at high centrifugal forces (Rayleigh–Taylor instability[16]) resulting in air bubbles that leave the receiving chamber which lowers the air counter-pressure.

Experiments and results

Physical effects relevant for the experiments

The centrifugo-pneumatic valve was characterized for a wide range of surface tensions, connection channel geometries and volumes of the receiving chamber. All experiments were observed with a stroboscopic setup[17] under rotation and burst frequencies were determined by increasing the centrifugal frequency in 1 Hz steps until liquid was observed in the receiving chamber (Fig. 2).

Three effects are considered for predicting the operating range of the centrifugo-pneumatic valve:

1. Pinning. Pinning of the meniscus arises due to the surface tension of the liquid at the sudden 3D-expansion of the narrow connection channel towards the receiving chamber. A 90° expansion angle is assumed for the side and bottom channel walls, while the top wall is defined by the lid and does not expand (0°). The associated pressure p_{cap} can be calculated by the integral theorem[18] according to eqn (1) and (2):

$$p_{cap} = -\frac{\sigma}{A}\sum_i \cos(\Theta_i) l_i \tag{1}$$

$$\Rightarrow p_{cap} = \sigma\left(\frac{2\sin\Theta}{w} + \frac{\sin\Theta}{d} - \frac{\cos\Theta}{d}\right) \tag{2}$$

where σ is the surface tension of the liquid, A, w and d are the cross-section area, width and depth of the rectangular narrow connection channel and Θ is the contact angle between liquid and substrate. In the presented experiments, the same material was used for substrate and lid. l_i is the projection of the liquid/solid interface line with the contact angle Θ_i on the channel's cross-section A.

2. Air compression. Air compression results in an increased pressure Δp_{air} in the receiving chamber due to intrusion of the meniscus (ideal gas law) (eqn (3)):

$$\Delta p_{air} = p_0 \frac{V_0}{V_0 - \Delta V} - p_0 \tag{3}$$

where p_0 is the ambient pressure (100 kPa), V_0 the volume of the receiving chamber and ΔV the air volume reduction due to the intruding meniscus.

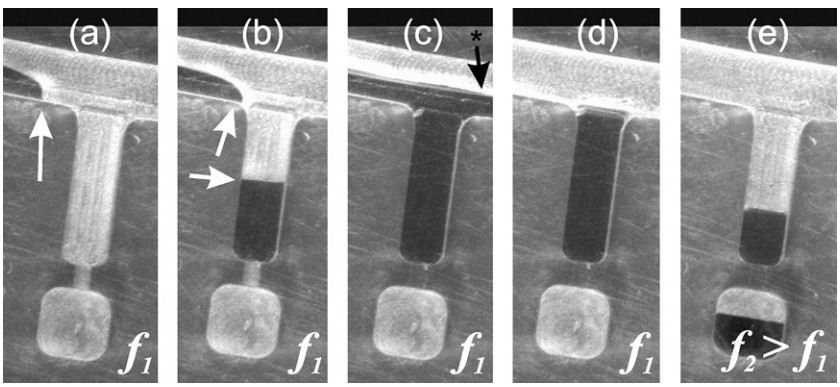

Fig. 2 Centrifugo-pneumatic valve observed by a stroboscopic measurement setup. The white arrows highlight the advancing liquid interface. (a, b) Liquid from the feed channel fills the metering channel at a metering rotational frequency f_1, (c, d) after the metering chamber is filled, excess liquid leaves *via* the overflow channel (c,*) thus defining a metered volume and (e) is transported into the receiving chamber at a higher burst frequency f_2. The liquid in these images is colored with ink for better visibility.

3. Rayleigh–Taylor instability. In order to fill the receiving chamber completely, the intruding liquid has to replace the air. Air can only escape through the channel through which the liquid enters. This happens when high centrifugal forces destabilize the liquid/air interface. The condition for an interface destabilization at a centrifugal frequency f_{RT} is given by eqn (4):[16]

$$f_{RT} = \frac{1}{\lambda_{crit}}\sqrt{\frac{\sigma}{W\rho}} \tag{4}$$

where λ_{crit} is a critical length of the interface, W is the radial position of the valve and ρ is the density of the liquid. It is noteworthy that this condition is independent of the plug length, thus permitting a complete emptying of the metering channel at decreasing plug length.

In order to quantify the valve, the burst frequency was defined as the centrifugal frequency at which liquid visibly enters the receiving chamber (optical limit of detection (LOD) in this setup: LOD = 0.2 μL). The Rayleigh–Taylor instability occurs at relatively high frequencies and enables complete emptying of the metering channel. For determining the burst pressure p_{burst}, a semi-empirical expression (eqn (5)) considering capillary and pneumatic pressure effects proved most effective:

$$\begin{aligned} p_{burst} &= Cp_{cap} + B + \Delta p_{air} \Rightarrow \\ (2\pi f_{burst})^2 \rho l R &= C\sigma\left(\frac{2\sin\Theta}{w} + \frac{\sin\Theta}{d} - \frac{\cos\Theta}{d}\right) \\ &\quad + B + p_0\left(\frac{V_0}{V_0 - \Delta V} - 1\right) \end{aligned} \tag{5}$$

where l is the length of the liquid plug (= length of the metering channel), R the mean radial position of the liquid plug and f_{burst} the burst frequency. The empirical constants C and B represent the experimental finding that the air pressure in the closed receiving chamber enhances the stability of the liquid/air interface and account for the specific geometry of the centrifugo-pneumatic valve. It should be noted that eqn (5) does not approach the pinning burst pressure p_{cap} for $V_0 \rightarrow \infty$. For a more detailed theoretical analysis, the dependency of C on V_0 for large V_0 has to be taken into account. However, for the observed realistic parameter space, this equation predicts the burst frequencies very well.

Results

Influence of the surface tension

First, the centrifugal burst frequency f_{burst} was measured for connection channels with w = 400 μm, d = 150 μm and liquids with different surface tensions, including varying Tween 20 concentrations (Sigma–Aldrich Laborchemikalien GmbH, Germany) and pure ethanol (Merck KgaA, Germany, ethanol pro analysi). The centrifugo-pneumatic valve reliably stopped all liquids (Fig. 3) with decreasing burst frequencies for decreasing surface tension, as expected from eqn (5). If residual liquid remained in the metering structure, a second step with a deceleration (*e.g.* to 10 Hz for water) and acceleration step (to 50 Hz) proved helpful. In order to quantify the pneumatic effect, the expected pinning pressure p_{cap} was plotted *vs.* the observed centrifugal burst pressure (calculated from f_{burst} according to eqn (5)). The result was fitted to the experimental data in the following variation of eqn (5):

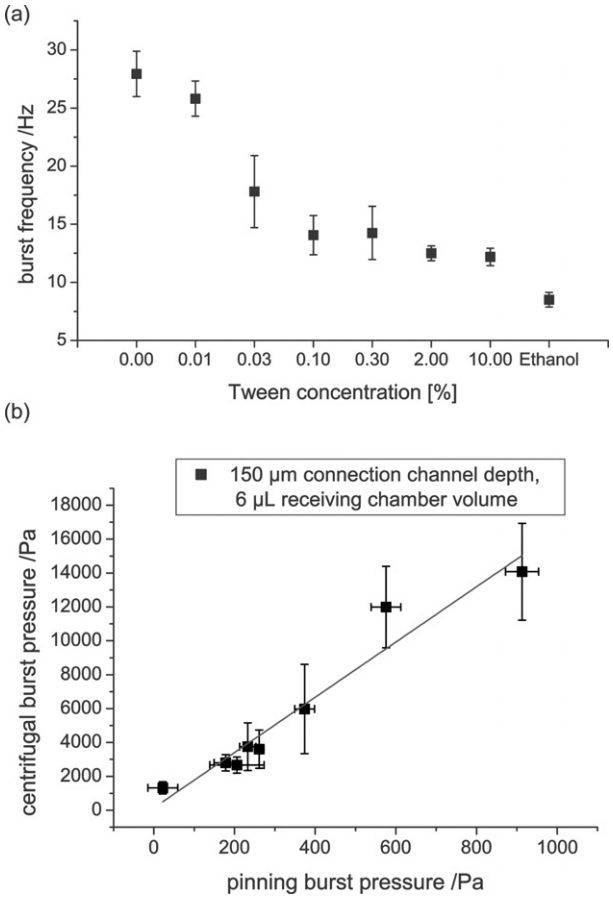

Fig. 3 Plots of the experimental burst frequencies for different liquids. (a) Burst frequencies for different Tween 20 concentrations and ethanol, the error bars represent one standard deviation (16 data points each). (b) Expected pinning pressure (eqn (2)) *vs.* observed centrifugal burst pressure for different surface tensions (experimental data as in plot (a)). The high slope shows the enhancement of the centrifugal burst pressure by the unvented receiving chamber. The line represents a fit to eqn (6).

$$p_{burst} = C\sigma\left(\frac{2\sin\Theta}{w} + \frac{\sin\Theta}{d} - \frac{\cos\Theta}{d}\right) + A(V_0) \tag{6}$$

where $A(V_0)$ includes the constant B and the air pressure term. The following fit parameters were found: $C = 16.3 \pm 1.7$, $A(V_0) = 144 \pm 722$ Pa (fit with Origin 6.1G, OriginLab Corp., Northampton, MA, USA). This shows the significant effect of the unvented receiving chamber, since a value of $C = 1$ would be expected for a simple pinning effect.

Values for the surface tension, the contact angles, and a movie of the burst can be found in ESI.†

Influence of the connection channel geometry

The influence of the connection channel geometry was also investigated by varying the connection channel depth at a constant width of 400 μm. The resulting data were fitted to eqn (6) (Fig. 4).

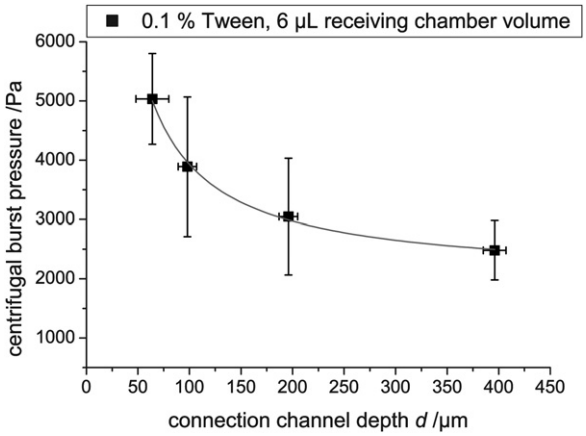

Fig. 4 Observed centrifugal burst pressures for different connection channel depths (bars represent one standard deviation, 4 data points each). The channel width w was 400 µm. The line represents a fit to eqn (6).

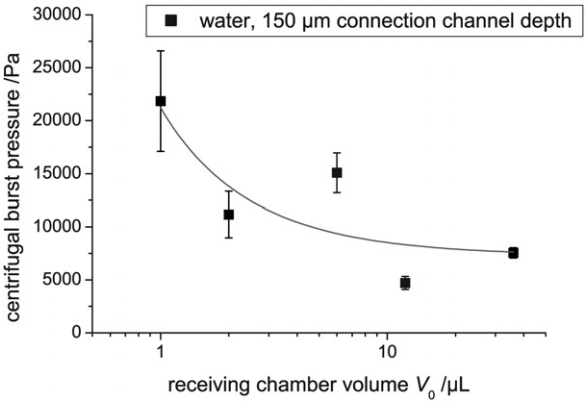

Fig. 5 Measured influence of the receiving chamber volume on the burst pressure. Squares represent measurements, bars one standard deviation (at least 10 data points each), and the line a fit based on eqn (7). The set target depth was 150 µm, however, due to prototyping tolerances, the valves with 2 and 12 µL volume had an average connection channel depth of 170 µm while the valves with 1, 6 and 36 µL volume had an average channel depth of 155 µm. This explains the variation in centrifugal burst pressures.

Fit parameters were found to be $C = 15.5 \pm 0.6$ and $A(V_0) = -768 \pm 169$ Pa which is consistent with the fit in Fig. 3. This shows that burst pressures for the centrifugo-pneumatic valve can be tuned by the connection channel geometry.

Influence of the receiving chamber volume

Since the enhanced stopping effect of the centrifugo-pneumatic valve is attributed to air compression, the compressible volume and thus the receiving chamber is also an important parameter. Therefore, the burst frequencies for chamber volumes V_0 between 1 and 36 µL were measured with pure water (Fig. 5). The result was fitted to the following variation of eqn (5):

$$p_{\text{burst}} = D(\sigma, \Theta, d) + p_0\left(\frac{V_0}{V_0 - \Delta V} - 1\right) \quad (7)$$

where the constant D includes the effects related to surface tension, contact angle and connection channel depth.

The fit resulted in the following parameters: $D = 7294 \pm 2542$ Pa and intruding liquid $\Delta V = 0.122 \pm 0.040$ µL, which is consistent with the previous findings, and the limit of detection ($\text{LOD}_{\Delta V} \leq 0.2$ µL). The discrepancies between the observed burst pressures for $V_0 = 1$, 6 and 36 µL compared to $V_0 = 2$ and 12 µL can be explained by prototyping tolerances: The structures with 1, 6 and 36 µL (test-disk 1) had an average connection channel depth d of 155 µm, whereas the structures with 2 and 12 µL (test-disk 2) had an average connection channel depth of 170 µm, lowering the burst pressure according to eqn (5).

The intrusion of small volumes of liquid prior to the burst is owed to the definition of the burst frequency which is determined by a visible amount of liquid in the receiving chamber. Liquid in the receiving chamber can probably be avoided altogether if a low metering frequency, *e.g.* 8 Hz for water, is chosen. According to eqn (5) and the experimentally determined values for the empirical constants, the compression of the connection channel volume (~0.04 µL) would be enough to stop the liquid, so the receiving chamber can stay completely dry during the metering step.

Materials & fabrication

The valving structures were micro-milled with a Minimill 3 (Minitech Machinery Corp., GA, USA) in a 4 mm cycloolefin-polymer (COP) disk (material from microfluidic ChipShop GmbH, Germany) using end mills with 0.4 mm and 1 mm diameter (F126.0040 and F113.0100, Gienger Industrie-Service, Switzerland). The disk was sealed with a two-layered foil as described previously.[19] Measurements were carried out on a centrifugal test stand with stroboscopic image acquisition.[17]

Conclusions

We have designed, fabricated and tested a novel valving structure for centrifugal microfluidic platforms that shows robust valving for a variety of liquids commonly used in biochemical assays (aqueous solutions containing detergents or ethanol) that are problematic for other passive valves due to the low surface tension and contact angle. The valve can be fabricated without micron-precise structures or local surface modifications and is easily implemented in low-cost microfluidic polymer substrates. The dependency of the burst frequency on the downstream volume of the microfluidic network makes it very useful at a blind (downstream) end of a microfluidic structure with sufficiently small downstream volume (verified for up to 36 µL downstream volume).

A series of centrifugo-pneumatic valves that branch off from a common feed channel can serve as a novel aliquoting structure with a unique advantage over existing metering structures: it requires no hydrophobic patches, works for highly wetting liquids and the metered volume is defined by a metering structure and not by the receiving chamber. This allows pre-storage of lyophilized or other reagents in the receiving chamber without changing the metered volumes. Additionally, since forwarding into the receiving chambers occurs simultaneously, all enzymatic reactions start at the same time. Also, the receiving chambers are not fluidically connected after aliquoting, thus preventing

cross-contamination between adjacent chambers. A precise aliquoting structure splitting a 105 μL volume into 16 aliquots with a CV of 3.0% (corresponding to the fabrication tolerance of ~20 μm in each dimension) was already tested with various liquids including highly wetting buffers (data not shown), proving the effectiveness of the centrifugo-pneumatic valve. Such a centrifugo-pneumatic valve based aliquoting structure is meant for point-of-care multiparameter- or panel-analysis. Examples are PCR genotyping or multiple colorimetric enzymatic reactions in clinical chemistry. Thus, the centrifugo-pneumatic valve is a valuable addition to the existing centrifugal microfluidic toolbox of unit operations for switching and metering.

Acknowledgements

We gratefully acknowledge financial support by the German Federal Ministry of Education and Research (project Zentrilab, grant number 16SV2347) and the European Union (project MagRSA, contract number 037957).

Notes and references

1 S. Haeberle and R. Zengerle, *Lab Chip*, 2007, **7**, 1094–1110.
2 A. P. Wong, M. Gupta, S. S. Shevkoplyas and G. M. Whitesides, *Lab Chip*, 2008, **8**, 2032–2037.
3 Y. K. Cho, J. G. Lee, J. M. Park, B. S. Lee, Y. Lee and C. Ko, *Lab Chip*, 2007, **7**, 565–573.
4 B. S. Lee, J. N. Lee, J. M. Park, J. G. Lee, S. Kim, Y. K. Cho and C. Ko, *Lab Chip*, 2009, **9**, 1548–1555.
5 J. Steigert, M. Grumann, M. Dube, W. Streule, L. Riegger, T. Brenner, P. Koltay, K. Mittmann, R. Zengerle and J. Ducrée, *Sens. Actuators, A*, 2006, **130–131**, 228–233.
6 J. Ducrée, S. Haeberle, S. Lutz, S. Pausch, F. von Stetten and R. Zengerle, *J. Micromech. Microeng.*, 2007, **17**, 103–115.
7 M. Madou, J. Zoval, G. Y. Jia, H. Kido, J. Kim and N. Kim, *Annu. Rev. Biomed. Eng.*, 2006, **8**, 601–628.
8 M. R. McNeely, M. K. Spute, A. R. Tusneem, and A. R. Oliphjant, *Proceedings of SPIE Microfluidic Devices and Systems II*, 1999, Santa Clara, 210–220.
9 G. Ekstrand, C. Holmquist, A. E. Örlefors, B. Hellman, A. Larsson, and P. Andersson, *Proceedings of Fourth International Conference on Micro Total Analysis Systems*, 2000, Enschede, 311–314.
10 D. C. Duffy, H. L. Gillis, J. Lin, N. F. Sheppard and G. J. Kellogg, *Anal. Chem.*, 1999, **71**, 4669–4678.
11 J. M. Chen, P. C. Huang and M. G. Lin, *Microfluid. Nanofluid.*, 2008, **4**, 427–437.
12 C. T. Schembri, T. L. Burd, A. R. Kopfsill, L. R. Shea and B. Braynin, *J. Autom. Chem.*, 1995, **17**, 99–104.
13 R. H. Liu, J. Bonanno, J. Yang, R. Lenigk and P. Grodzinski, *Sens. Actuators, B*, 2004, **98**, 328–336.
14 J. M. Park, Y. K. Cho, B. S. Lee, J. G. Lee and C. Ko, *Lab Chip*, 2007, **7**, 557–564.
15 J. Kim, H. Kido, R. H. Rangel and M. J. Madou, *Sens. Actuators, B*, 2008, **128**, 613–621.
16 An overview of Rayleigh–Taylor instability: D. H. Sharp, *Phys. D*, 1984, **12**, 3–18.
17 M. Grumann, T. Brenner, C. Beer, R. Zengerle and J. Ducrée, *Rev. Sci. Instrum.*, 2005, **76**, 025101.
18 D. Langbein, in *Capillary surfaces: shape, stability, dynamics, in particular under weightlessness*, Springer-Verlag, Heidelberg, Germany, 2002, ch. 3, p. 47.
19 J. Steigert, S. Haeberle, T. Brenner, C. Muller, C. P. Steinert, P. Koltay, N. Gottschlich, H. Reinecke, J. Ruhe, R. Zengerle and J. Ducrée, *J. Micromech. Microeng.*, 2007, **17**, 333–341.